Hard probes in isobar collisions & nuclear structures

Intersection of nuclear structure and high-energy nuclear collisions
INT 23-1a program, Week 2, Feb 1, 2023

Weiyao Ke, Los Alamos National Laboratory

- Hard probes in heavy-ion collisions
- Different scaling of hard and soft particle production.
- Sensitivity of isospin dependent probes W^-/W^+ to neutron skin.
- Improving the Monte-Carlo Glauber modeling in isobar collisions.

Particle productions in heavy-ion collisions

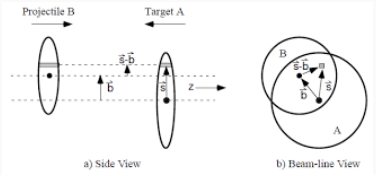

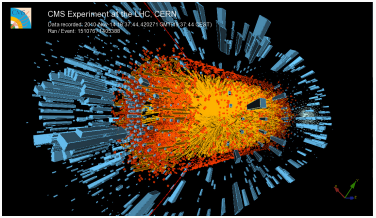

- High energy collisions: $\gamma \gg 1$. Spatial information in z highly compressed.
- Initial particle productions are localized in transverse plane. Nuclear geometry only enters in the form of thickness functions

$$T_A(x_\perp) = \int \rho_A(x_\perp, z) dz$$

$$T_B(x_\perp) = \int \rho_B(x_\perp, z) dz$$

From geometry to cross sections: the Glauber model

AB cross sections from NN cross sections and thickness functions

$$\begin{aligned}\sigma_{AB} &= \int d^2b \left[1 - \left[1 - \sigma_{NN} \frac{\int_{x_\perp} d^2 T_A(x_\perp) T_B(b - x_\perp)}{AB}\right]^{AB}\right] \\ &\approx \int d^2b \left[1 - \exp\left\{-\int d^2x_\perp \sigma_{NN\to X} T_A(x_\perp) T_B(b - x_\perp)\right\}\right]\end{aligned}$$

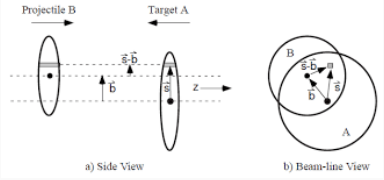

- If X is a frequent process, σ_{AB} follows the geometric area.
- If X is a rare process, such as high-p_T jets, weak bosons

$$\sigma_{AB\to X} = \int d^2b \int d^2x_\perp \sigma_{NN\to X} T_A(x_\perp) T_B(b - x_\perp)$$

Scaling of bulk (soft) hadron production

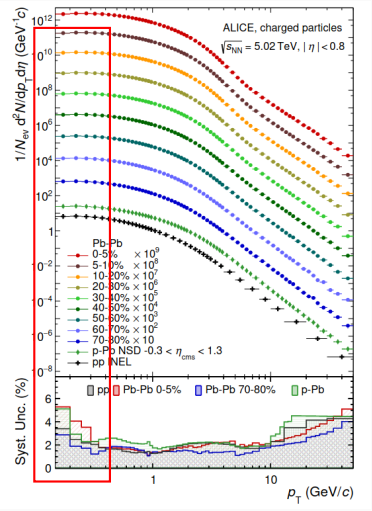

- $p_T \lesssim 1$ GeV. High multiplicity, apprixmately goes like number of participants N_{part}, $\int_x T_A(x)(1 - e^{-\sigma_{NN} T_B(b-)}) + T_B(b-x)(1 - e^{-\sigma_{NN} T_A(x)})$
- Charged particle multiplicity strongly correlates with impact parameter, events classified by centrality.
- Bulk particles at middle rapitidy are produced from small-x content of the nucleus, isospin insensitive.

Final-state dynamics contributing to particle production

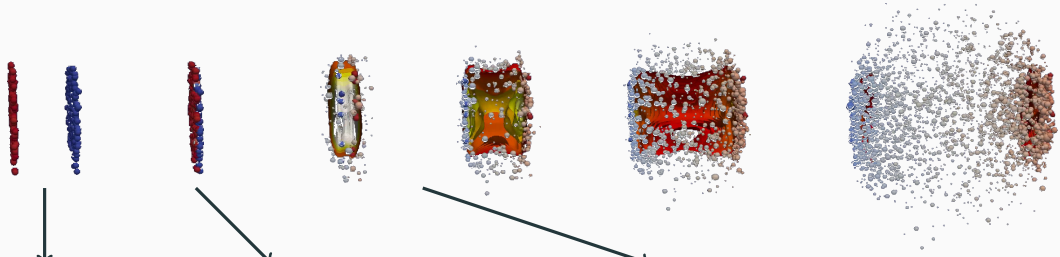

Nuclear structure parameters
$T_A(x_\perp; R, a, \beta \cdots)$

Initial energy deposition.
A major source of uncertainty.

- $T_A(x)$, $T_B(x) \to e(x_\perp, \eta_s)$.
- Granularity, initial flow, $\cdots$.

Dynamical response

- Geometry $\to$ momentum-space information, entropy production.
- Relies on transport parameters.

Current accuracy for **a single system** $\sim 5 - 10\%$
from global fits Jetscaoe PRC103(2021)054904

Production of hard probes in HIC

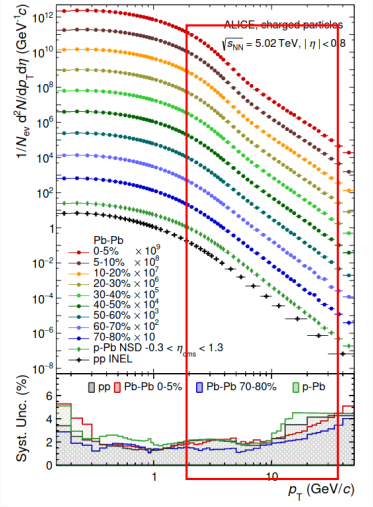

ALICE Pb-Pb, pp @ 5.02 TeV

- High-p_T processes, well-known production mechanism with high accuracy in pp.

$$\sigma_{\mathrm{NN}\to\mathrm{h}} = f_{i/N} f_{j/N} \otimes \hat{\sigma}_{ij\to k} \otimes D_{h/k}(z)$$

- A traditional observable: nuclear modification factor

$$R_{AA} = \frac{1}{\langle T_{AA} \rangle} \frac{dN_{\mathrm{AA}\to\mathrm{h}}}{d\sigma_{\mathrm{pp}\to\mathrm{h}}}$$

- $T_{AA} = N_{\mathrm{coll}}/\sigma_{pp,inel}$. If AA are independent superposition of free NN collisions, then $R_{AA} = 1$.

Production of hard probes in HIC

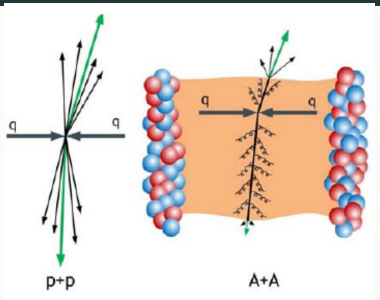

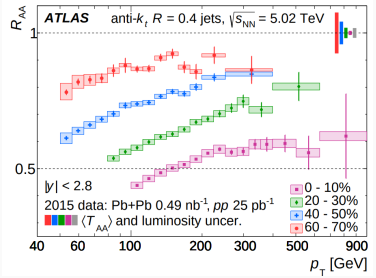

ATLAS jet R_{AA}, PLB790 (2019)108

- High-p_T processes, well-known production mechanism with high accuracy in pp.

$$\sigma_{\mathrm{NN}\to\mathrm{h}} = f_{i/N} f_{j/N} \otimes \hat{\sigma}_{ij\to k} \otimes D_{h/k}(z)$$

- A traditional observable: nuclear modification factor

$$R_{AA} = \frac{1}{\langle T_{AA} \rangle} \frac{dN_{\mathrm{AA}\to\mathrm{h}}}{d\sigma_{\mathrm{pp}\to\mathrm{h}}}$$

- $T_{AA} = N_{\mathrm{coll}}/\sigma_{pp,inel}$. If AA are independent superposition of free NN collisions, then $R_{AA} = 1$.

- Colorful probes (high-p_T hadrons, jets) are suppressed from parton energy loss / modified fragmentations in QGP modifications $D_{h/k}(z; T(x), u^{\mu}(x))$ in QGP.

Probing fireball geometry with jets

- Jet probes path-length integrated QGP fireball information.
- In a weakly-coupled picture, parton energy loss in QGP (jet energy loss more involved)

$$\Delta E = \underbrace{\frac{C_R}{4}\int_0^L \alpha_s(ET)\ln\frac{ET}{m_D^2}m_D^2 d\tau}_{\text{Collisional}} + \underbrace{\alpha_s C_R\int_0^L \hat{q}_g(\tau)\tau d\tau \ln\frac{2E}{m_D^2\tau}+\cdots}_{\text{GLV type radiative energy loss}}$$

- Average over jet production locations ($\propto T_A(x_\perp)T_B(x_\perp)$) and orientations ϕ.
- Correlating high-p_T hadron/jet with soft-particle event plane $\Rightarrow$ finite high-p_T v_n.

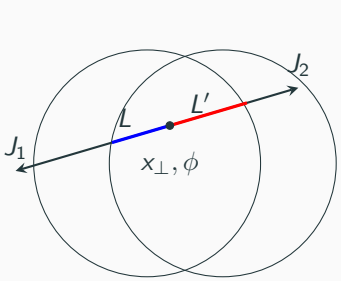

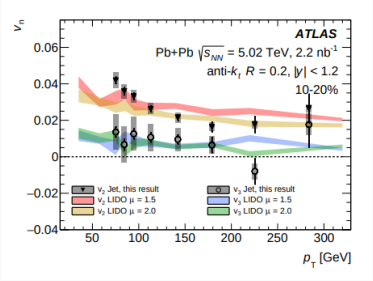

ATLAS: jet v_2, v_3.

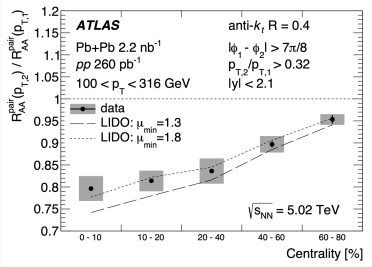

Subleading/leading jet R_{AA} $\rightarrow$ consider an isobar ratio?

Colorless probes: $W^{\pm}, Z$ bosons

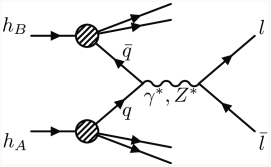

Lepton	$2c_V$	$2c_A$	Quark	$2c_V$	$2c_A$
ν_e, ν_μ, ν_τ	1	1	u, c, t	$1 - \frac{8}{3}\sin^2\theta_W$	1
e, μ, τ	$-1 + 4\sin^2\theta_W$	-1	d, s, b	$-1 + \frac{4}{3}\sin^2\theta_W$	-1

W, Z do not interact with QGP, all modifications come from initial states.

$$\sigma_{AB\to W,Z}(x_\perp) = \phi_{i/A}(x_1, Q^2; x_\perp)\phi_{j/B}(x_2, Q^2; b - x_\perp) \otimes \hat{\sigma}_{ij\to W,Z} \otimes \Gamma_{W\to l\nu_l}, \Gamma_{Z\to l^+l^-}$$

- Local parton luminosity $\phi_{i/A}\phi_{j/B}$.

$$\phi_{i/A}(x_1, Q^2; x_\perp) \to T_{p/A}(x_\perp) f^A_{i/p}(x_1, Q^2; T_A(x_\perp)) + T_{n/A}(x_\perp) f^A_{i/n}(x_1, Q^2; T_A(x_\perp))$$

  $f^A_{i/p}$ and $f^A_{i/n}$ related by isospin symmetry.

- Nuclear PDFs differ from free proton PDF. Modifications are often assumed to only depend on local thickness. Though most parametrizations only have $f^A_{i/p}(x_1, Q^2; A)$.

- How much do nuclear PDF uncertainty cancels in isobar ratios?

Colorless probes: $W^{\pm}, Z$ bosons

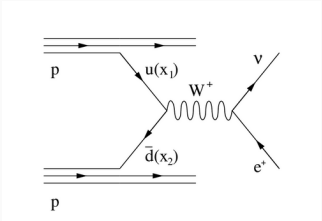

$$\begin{bmatrix} |V_{ud}| & |V_{us}| & |V_{ub}| \\ |V_{cd}| & |V_{cs}| & |V_{cb}| \\ |V_{td}| & |V_{ts}| & |V_{tb}| \end{bmatrix} = \begin{bmatrix} 0.97370 \pm 0.00014 & 0.2245 \pm 0.0008 & 0.00382 \pm 0.00024 \\ 0.221 \pm 0.004 & 0.987 \pm 0.011 & 0.0410 \pm 0.0014 \\ 0.0080 \pm 0.0003 & 0.0388 \pm 0.0011 & 1.013 \pm 0.030 \end{bmatrix}$$

W, Z do not interact with QGP, all modifications come from initial states.

$$\sigma_{AB\to W,Z}(x_\perp) = \phi_{i/A}(x_1, Q^2; x_\perp)\phi_{j/B}(x_2, Q^2; b - x_\perp) \otimes \hat{\sigma}_{ij\to W,Z} \otimes \Gamma_{W\to l\nu_l}, \Gamma_{Z\to l^+l^-}$$

- Local parton luminosity $\phi_{i/A}\phi_{j/B}$.

$$\phi_{i/A}(x_1, Q^2; x_\perp) \to T_{p/A}(x_\perp) f^A_{i/p}(x_1, Q^2; T_A(x_\perp)) + T_{n/A}(x_\perp) f^A_{i/n}(x_1, Q^2; T_A(x_\perp))$$

  $f^A_{i/p}$ and $f^A_{i/n}$ related by isospin symmetry.

- Nuclear PDFs differ from free proton PDF. Modifications are often assumed to only depend on local thickness. Though most parametrizations only have $f^A_{i/p}(x_1, Q^2; A)$.

- How much do nuclear PDF uncertainty cancels in isobar ratios?

NLO $W^{\pm}, Z$ cross section

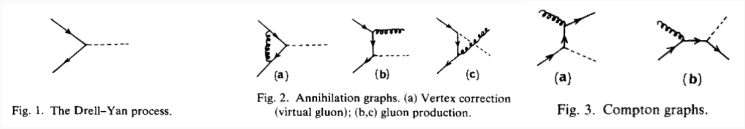

Fig. 1. The Drell–Yan process.

Fig. 2. Annihilation graphs. (a) Vertex correction (virtual gluon); (b,c) gluon production.

Fig. 3. Compton graphs.

CT14NLO proton PDF + NLO hard cross-section.

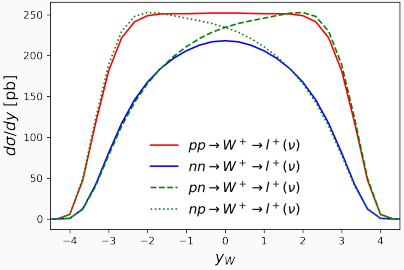

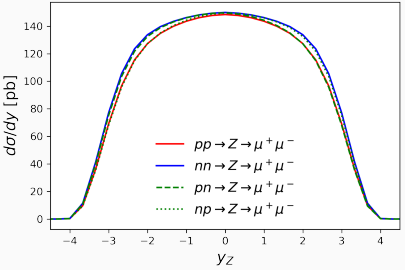

Weak boson production in Pb Pb at 5.02 TeV

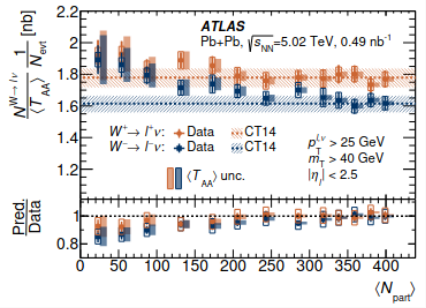

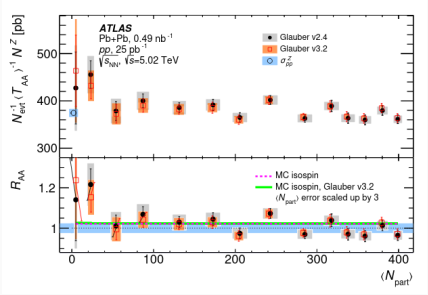

ATLAS: EPJC79(2019)935, PLB802(2020)135262

- Already at the level showing deviations of the default Glauber model. Also note the large $\langle T_{AA} \rangle$ uncertainty.
- $W^{\pm}$ can be sensitive to neutron skin.

Weak boson production in Pb Pb at 5.02 TeV

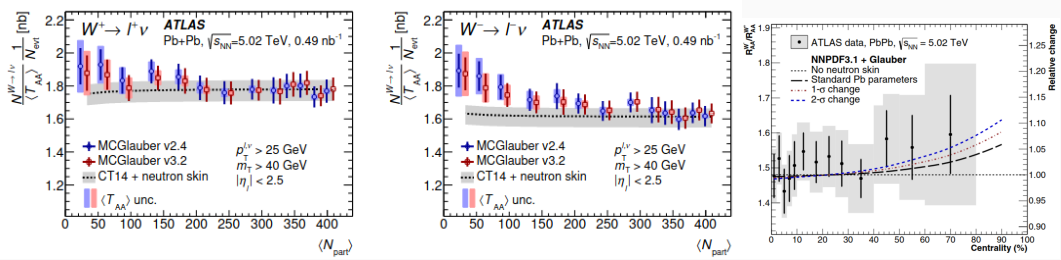

Neutron skin effect calculations: H. Paukkunen PLB745(2015)73-78 (left); F. Jonas, C. Loizides PRC104(2021)044905 (right).

- Already at the level showing deviations of the default Glauber model. Also note the large $\langle T_{AA} \rangle$ uncertainty.
- $W^{\pm}$ can be sensitive to neutron skin.

The TRENTo model[1]

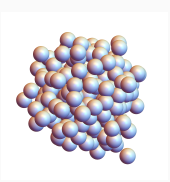

^{208}Pb

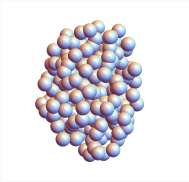

^{238}U

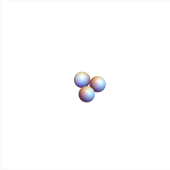

^{3}He

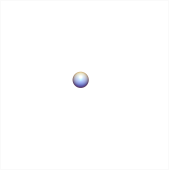

p

- Heavy nucleus: $\frac{A}{\mathcal{N}} \frac{1}{1+\exp\left(\frac{r-R(\theta,\phi;\beta_n)}{a}\right)}$ deformation parameters from [Atom.Data Nucl.Data Tabl. 109-110 (2016) 1].
- min $r_{ij} > d_{\text{min}}$ to mimic short-range repulsion.
- Light nuclei: load samples of nuclear configurations from nuclear structure calculations, e.g., ^{3}He [PLB 680, 225–230 (2009)].

This study includes β_3 deformation and two sets of WS parameters $(R, a, \beta_2, \beta_3, ...)$, $\rho_p \neq \rho_n$ + evaluation of different types of binary collisions N_{pp}, N_{pn}, N_{nn}.

[1] TRENTo: JS Moreland, JE Bernhard, SA Bass, PRC 92, 011901 (2015), http://qcd.phy.duke.edu/trento/index.html

Nucleon profile and N-N inelastic cross section

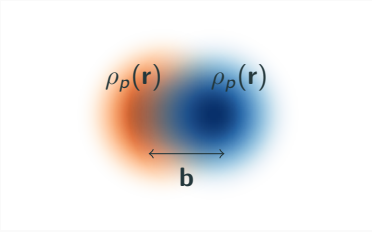

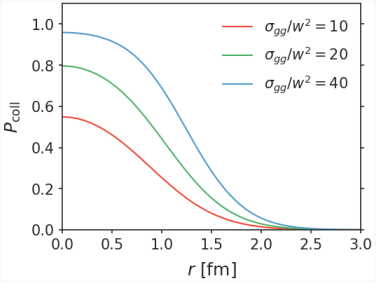

Nucleon model #1: Gaussian proton

$$\rho_p(\mathbf{r}, z) = \frac{e^{-\frac{\mathbf{r}^2+z^2}{2w^2}}}{(2\pi w)^{3/2}} \xrightarrow{\int dz} \rho_p(\mathbf{r}) = \frac{e^{-\frac{r^2}{2w^2}}}{2\pi w^2}$$

Probability of inelastic collisions at fixed impact parameter.

$$\begin{aligned} T_{pp}(b) &= \int \rho_p(\mathbf{r}-\mathbf{b}/2)\rho_p(\mathbf{r}+\mathbf{b}/2)d^2\mathbf{r} \\ P_{\rm coll}(b) &= 1-\exp\left\{-\sigma_{gg}\, T_{pp}(b)\right\} \end{aligned}$$

σ_{gg}: effective opacity parameter tuned to reproduce $\sigma_{pp}^{\rm inel}(\sqrt{s})$

$$\sigma_{pp}^{\rm inel}\sqrt{s} = \int P_{\rm coll}(\mathbf{b}; \sigma_{gg}(\sqrt{s}))d\mathbf{b}^2$$

Nucleon profile and N-N inelastic cross section

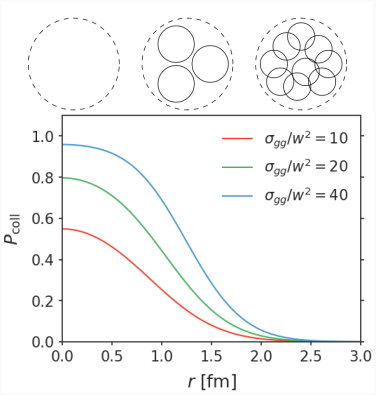

Nucleon model #2: with substructures [JS moreland, JE Bernhard, SA Bass, PRC 101, 024911]

$$\rho_p(r) = \frac{1}{N}\sum_{i=1}^{N} \frac{e^{-\frac{(r-r_i-R_{\rm cm})^2}{2w_c^2}}}{2\pi w_c^2}, r_i \sim \frac{e^{-\frac{r_i^2}{2w'^2}}}{2\pi w'^2}$$

$R_{\rm cm}$ fix the center of mass.

σ_{gg} solved by Monte Carlo integration to reproduce $\sigma_{pp}^{\rm inel}(\sqrt{s})$.

Binary collisions and fluctuating participants density

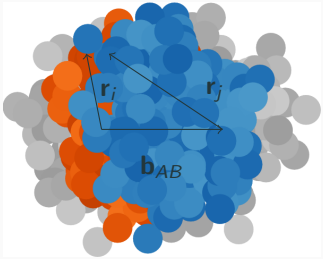

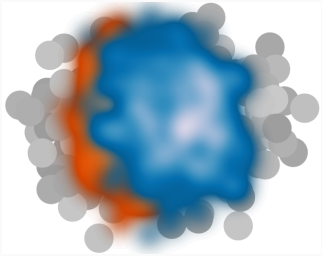

- Participant nucleons determined by sampling binary collision probability $P_{\mathrm{coll}}(b = |\mathbf{r}_j - \mathbf{b}_{AB} - \mathbf{r}_i|)$.
- Fluctuating participant density:

$$T_{A \text{ or } B}(\mathbf{r}) = \sum_{i \in \mathrm{Part.\ } A \text{ or } B} \gamma_i \rho_p(\mathbf{r} - \mathbf{r}_i)$$

- $P(\gamma_i) \propto \gamma^{k-1} e^{-k\gamma}$. Emulate fluctuation in *pp* measurement, can change with kinematic cuts!

Energy density production at mid-rapidity

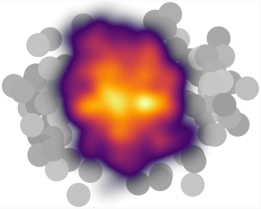

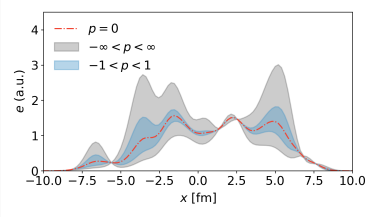

$$\frac{dE_T}{dx_\perp^2\, d\eta_s}(x_\perp, \eta_s = 0) = \mathrm{Norm} \times f(T_A(x_\perp), T_B(x_\perp))$$

TRENTo assumes

$$f(T_A, T_B) = \left(\frac{T_A^p + T_B^p}{2}\right)^{1/p}$$

known as "generalized mean" (p-mean) ansatz.

A motivation of using p-mean

p-mean is "homogeneous" $f(kT_A, kT_B) = kf(T_A, T_B)$.
Binary collisions $(T_A T_B)$ is not.

Side view	Beam view	ε_2	$N_{\rm part}$	$N_{\rm coll}$
U tip-tip U	U	smaller	equal	larger
U side-side U	U	larger	equal	smaller

If $N_{\rm coll}$ involved, fine binning of $N_{\rm ch}$ should differentiate ϵ_2 ▷.

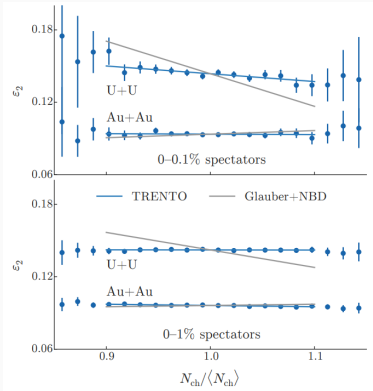

[JS Moreland, JE Bernhard, SA Bass, PRC 92, 011901 (2015)]

p-mean is a class of energy deposition consistent with this observation.

Two-component Glauber $N_{\rm ch} \propto (1-x)N_{\rm part} + xN_{\rm coll}$ is not consistent.

Connections to scaling of other models

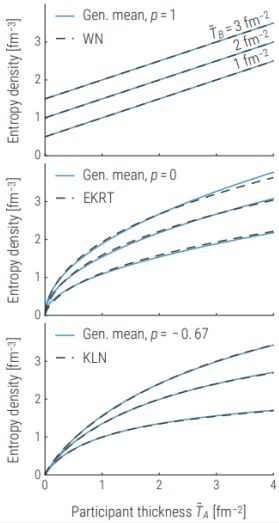

- Wounded nucleon model

$$\frac{dS}{dy\, d^2r_\perp} \propto \tilde{T}_A + \tilde{T}_B$$

- EKRT model PRC 93, 024907 (2016)
  after brief free streaming phase

$$\frac{dE_T}{dy\, d^2r_\perp} \sim \frac{K_{\mathrm{sat}}}{\pi} p_{\mathrm{sat}}^3(K_{\mathrm{sat}}, \beta; T_A, T_B)$$

- KLN model PRC 75, 034905 (2007)

$$\frac{dN_g}{dy\, d^2r_\perp} \sim Q_{s,\mathrm{min}}^2 \left[2 + \log\left(\frac{Q_{s,\mathrm{max}}^2}{Q_{s,\mathrm{min}}^2}\right)\right]$$

[JS Moreland]

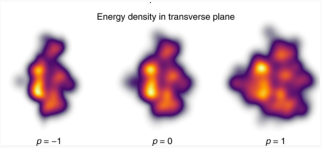

Still, only a subclass of exisiting models.

Connections to scaling of other models

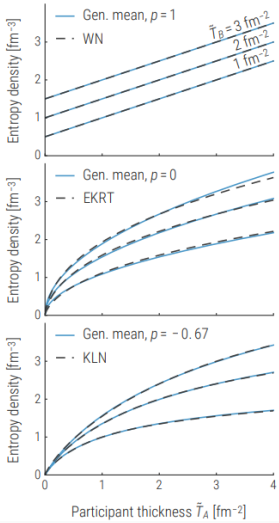

- Wounded nucleon model

$$\frac{dS}{dy\,d^2r_\perp} \propto \tilde{T}_A + \tilde{T}_B$$

- EKRT model PRC 93, 024907 (2016)

after brief free streaming phase

$$\frac{dE_T}{dy\,d^2r_\perp} \sim \frac{K_{\rm sat}}{\pi} p_{\rm sat}^3(K_{\rm sat}, \beta; T_A, T_B)$$

- KLN model PRC 75, 034905 (2007)

$$\frac{dN_g}{dy\,d^2r_\perp} \sim Q_{s,\rm min}^2 \left[2 + \log\left(\frac{Q_{s,\rm max}^2}{Q_{s,\rm min}^2}\right)\right]$$

[JS Moreland]

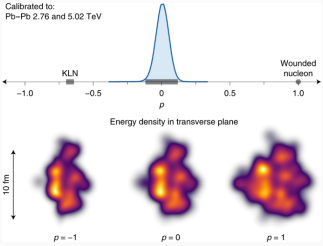

Bayesian analysis PbPb at LHC [Duke PRC 94 024907].

Variation of Woods-Saxon parameters

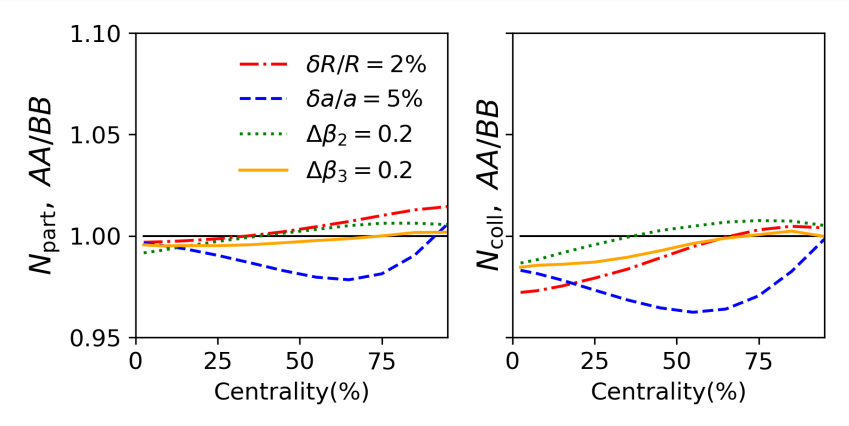

- Number of binary collision very sensitive to diffuseness and radius.
- In general, $N_{\rm coll}$ displays larger variation than $N_{\rm part}$.

Differentiating N_{pp}, N_{pn}, N_{nn} when $\rho_n \neq \rho_p$

Table 2: The WS parameterizations (radius parameter R and diffuseness parameter a) of proton and neutron (and nucleon) density distributions for ^{96}Ru and ^{96}Zr, matching to the corresponding $\langle r\rangle$ and $\langle r^2\rangle$ from the DFT-calculated spherical densities with SLy4 skyrme parameter set [1, 25]. The WS parameterization of nucleon density assuming a quadrupole deformity parameter $\beta_2 = 0.16$ and matching to the spherical DFT density is also listed. All quoted numbers are in fm.

		^{96}Ru		^{96}Zr	
		R	a	R	a
$\beta_2 = 0$	p	5.060	0.493	4.915	0.521
	n	5.075	0.505	5.015	0.574
	p+n	5.067	0.500	4.965	0.556
$\beta_2 = 0.16$	p	5.053	0.480	4.912	0.508
	n	5.073	0.490	5.007	0.564
	p+n	5.065	0.485	4.961	0.544

H.J. Xu et al., PLB819(2021)136453

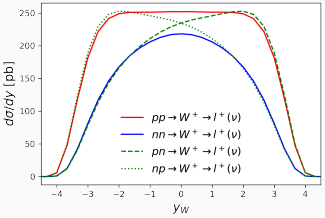

$\Leftrightarrow$

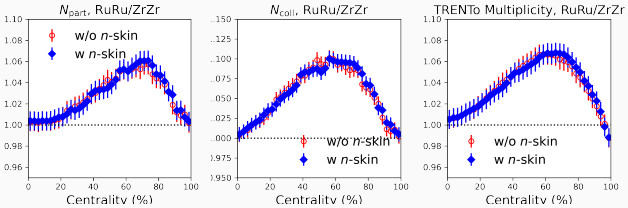

- Parameter sets w/ and w/o neutron skin gives identical $N_{\rm part}$/multiplicity, $N_{\rm coll}$ v.s. centrality.
- Deviations from unity coming from R, a.

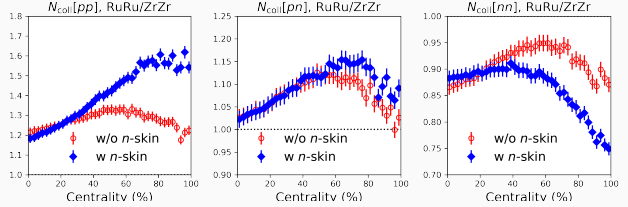

- Neutron-skin-sensitive quantity: N_{pp}, N_{pn}, N_{nn}

Centrality dependent weak boson production

For an event-averaged collision with $\langle N_{pp} \rangle$, $\langle N_{pn} \rangle$, $\langle N_{np} \rangle$, $\langle N_{nn} \rangle$,

$$\frac{d\sigma_{W^+}}{dMdy} = \langle N_{pp} \rangle \frac{d\sigma_{pp\to W^+}}{dy} + \langle N_{pn} \rangle \frac{d\sigma_{pn\to W^+}}{dMdy} + \langle N_{np} \rangle \frac{d\sigma_{np\to W^+}}{dMdy} + \langle N_{nn} \rangle \frac{d\sigma_{nn\to W^+}}{dMdy}$$

Including decay width for $W \to e\nu_e, \mu\nu_\mu$ and $Z \to e^+e^-, \mu^+\mu^-$, then integrated over the resonance peak (narrow resonance approximation formula from PRD69(2004)094008).

$$\frac{d\sigma_{W^\pm \to l\nu_l}}{dy} \approx [3.327\ \mathrm{GeV}] \times \frac{d\sigma_{W^\pm}}{dMdy}|_{M=m_W},$$
$$\frac{d\sigma_{Z\to l^+l^-}}{dy} \approx [3.919\ \mathrm{GeV}] \times \frac{d\sigma_Z}{dMdy}|_{M=m_Z}.$$

Nuclear PDF uncertainty

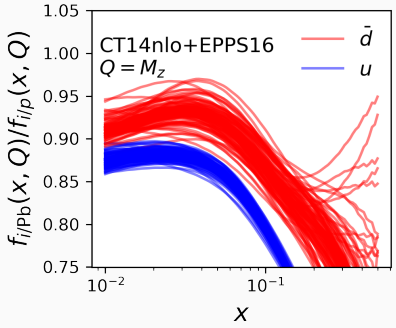

Proton PDF: CT14nlo, S. Dulat et al., PRD93(2016)033006.
Nuclear PDF: EPPS16, K. Eskola et al., EPJC77(2017)163.

- A major uncertainty for hard process calculation in AA is the nuclear PDF uncertainty.
- In $R_{AA} = \frac{\sigma_{AA\to Z}}{\langle N_{\mathrm{coll}}\rangle \sigma_{pp\to Z}}$, about 10% uncertainty. Furthermore, nuclear PDF modulations can be impact-parameter dependent, not included in EPPS16.
- Nuclear PDF are often assumed to be isospin independent $f_{u/p} = f_(d/n)$. Modifications only depends on A or the thickness (deformation?).

Reducing nPDF uncertainty by taking isobar ratio $(W, Z)_{AA/BB}$

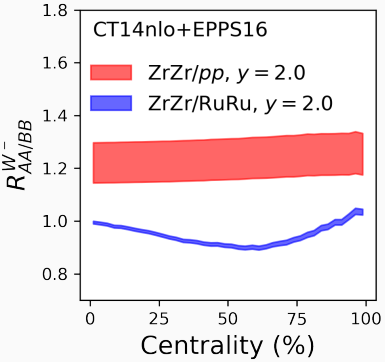

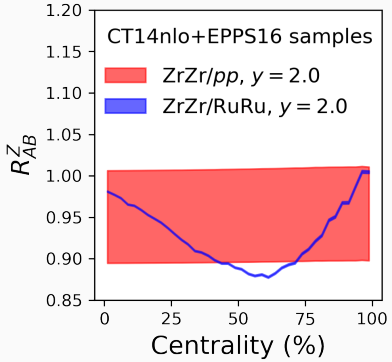

- If there is only A dependence, nPDF uncertainty almost "cancels" in isobar ratio: $\frac{\sigma_{\mathrm{RuRu}\to Z}}{\sigma_{\mathrm{ZrZr}\to Z}}$.
- What about impact-parameter/thickness dependent nPDF?

Vary neutron skin

Two crude ways to introduce neutron skin, just to estimate the sensitivity:

1. Change the Woods-Saxon diffuseness parameter $a_p = a - \delta a/2$, $a_n = a + \delta a/2$.
   Assume $\delta a = \frac{N-Z}{A} \times 0.8$ fm, corresponding to $\sqrt{\langle r_n^2 \rangle} - \sqrt{\langle r_p^2 \rangle} \approx$ 0.231 fm for ^{208}Pb.

2. Or, change the Woods-Saxon R parameter $R_p = R - \delta R/2$, $R_n = R + \delta R/2$.
   $\delta R = \frac{N-Z}{A} \times \delta R_0$ tuned to maintain the same neutron skin for each nucleus.

Available isobar pairs

A	isobars	A	isobars	A	isobars	A	isobars	A	isobars	A	isobars
36	Ar, S	80	Se, Kr	106	Pd, Cd	124	Sn, Te, Xe	148	Nd, Sm	174	Yb, Hf
40	Ca, Ar	84	Kr, Sr, Mo	108	Pd, Cd	126	Te, Xe	150	Nd, Sm	176	Yb, Lu, Hf
46	Ca, Ti	86	Kr, Sr	110	Pd, Cd	128	Te, Xe	152	Sm, Gd	180	Hf, W
48	Ca, Ti	87	Rb, Sr	112	Cd, Sn	130	Te, Xe, Ba	154	Sm, Gd	184	W, Os
50	Ti, V, Cr	92	Zr, Nb, Mo	113	Cd, In	132	Xe, Ba	156	Gd,Dy	186	W, Os
54	Cr, Fe	94	Zr, Mo	114	Cd, Sn	134	Xe, Ba	158	Gd,Dy	187	Re, Os
64	Ni, Zn	96	Zr, Mo, Ru	115	In, Sn	136	Xe, Ba, Ce	160	Gd,Dy	190	Os, Pt
70	Zn, Ge	98	Mo, Ru	116	Cd, Sn	138	Ba, La, Ce	162	Dy,Er	192	Os, Pt
74	Ge, Se	100	Mo, Ru	120	Sn, Te	142	Ce, Nd	164	Dy,Er	196	Pt, Hg
76	Ge, Se	102	Ru, Pd	122	Sn, Te	144	Nd, Sm	168	Er,Yb	198	Pt, Hg
78	Se, Kr	104	Ru, Pd	123	Sb, Te	146	Nd, Sm	170	Er,Yb	204	Hg, Pb

Getting more realistic: HL-LHC luminosity projections

Future physics opportunities for high-density QCD at the LHC with heavy-ion and proton beams. CERN-LPCC-2018-07.

Table 5: Parameters and performance for a range of light nuclei with an optimistic value of the scaling parameter $p = 1.9$ in (5).

	$^{16}O^{8+}$	$^{40}Ar^{18+}$	$^{40}Ca^{20+}$	$^{78}Kr^{36+}$	$^{129}Xe^{54+}$	$^{208}Pb^{82+}$
γ	3760.	3390.	3760.	3470.	3150.	2960.
$\sqrt{s_{NN}}$/TeV	7.	6.3	7.	6.46	5.86	5.52
σ_{had}/b	1.41	2.6	2.6	4.06	5.67	7.8
σ_{BFPP}/b	2.36×10^{-5}	0.00688	0.0144	0.88	15.	280.
σ_{EMD}/b	0.0738	1.24	1.57	12.2	51.8	220.
σ_{tot}/b	1.48	3.85	4.18	17.1	72.5	508.
N_b	1.58×10^{10}	3.39×10^{9}	2.77×10^{9}	9.08×10^{8}	4.2×10^{8}	1.9×10^{8}
ϵ_{xn}/μm	2.	1.8	2.	1.85	1.67	1.58
f_{IBS}/(m Hz)	0.168	0.164	0.184	0.18	0.17	0.167
W_b/MJ	175.	84.3	76.6	45.2	31.4	21.5
$L_{AA0}/\text{cm}^{-2}s^{-1}$	9.43×10^{31}	4.33×10^{30}	2.9×10^{30}	3.11×10^{29}	6.66×10^{28}	1.36×10^{28}
$L_{NN0}/\text{cm}^{-2}s^{-1}$	2.41×10^{34}	6.93×10^{33}	4.64×10^{33}	1.89×10^{33}	1.11×10^{33}	5.88×10^{32}
P_{BFPP}/W	0.0199	0.601	0.935	11.	60.6	350.
P_{EMD1}/W	32.	55.6	52.2	78.3	107.	141.
τ_{LB}/h	6.45	11.6	13.1	9.74	4.96	1.57
T_{opt}/h	5.68	7.62	8.08	6.98	4.98	2.8
$\langle L_{AA} \rangle \text{ cm}^{-2}s^{-1}$	4.54×10^{31}	2.45×10^{30}	1.69×10^{30}	1.68×10^{29}	2.95×10^{28}	3.8×10^{27}
$\langle L_{NN} \rangle \text{ cm}^{-2}s^{-1}$	1.16×10^{34}	3.93×10^{33}	2.71×10^{33}	1.02×10^{33}	4.91×10^{32}	1.64×10^{32}
$\int_{month} L_{AA}$ dt/nb^{-1}	5.89×10^{4}	3180.	2190.	218.	38.2	4.92
$\int_{month} L_{NN}$ dt/pb^{-1}	1.51×10^{4}	5090.	3510.	1330.	636.	213.
R_{had}/kHz	1.33×10^{5}	1.12×10^{4}	7540.	1260.	378.	106.
μ	10.6	0.893	0.598	0.1	0.03	0.00842

Luminosity quickly drops with A

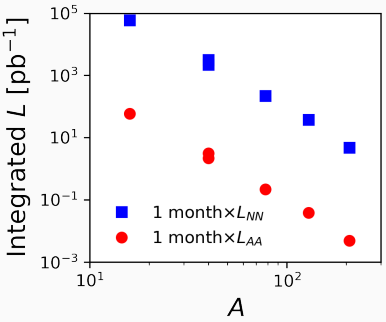

Getting more realistic: HL-LHC luminosity projections

Future physics opportunities for high-density QCD at the LHC with heavy-ion and proton beams. CERN-LPCC-2018-07.

Table 5: Parameters and performance for a range of light nuclei with an optimistic value of the scaling parameter $p = 1.9$ in (5).

	$^{16}O^{8+}$	$^{40}Ar^{18+}$	$^{40}Ca^{20+}$	$^{78}Kr^{36+}$	$^{129}Xe^{54+}$	$^{208}Pb^{82+}$
γ	3760.	3390.	3760.	3470.	3150.	2960.
$\sqrt{s_{NN}}$/TeV	7.	6.3	7.	6.46	5.86	5.52
σ_{had}/b	1.41	2.6	2.6	4.06	5.67	7.8
σ_{BFPP}/b	2.36×10^{-5}	0.00688	0.0144	0.88	15.	280.
σ_{EMD}/b	0.0738	1.24	1.57	12.2	51.8	220.
σ_{tot}/b	1.48	3.85	4.18	17.1	72.5	508.
N_b	1.58×10^{10}	3.39×10^{9}	2.77×10^{9}	9.08×10^{8}	4.2×10^{8}	1.9×10^{8}
ϵ_{xn}/μm	2.	1.8	2.	1.85	1.67	1.58
f_{IBS}/(m Hz)	0.168	0.164	0.184	0.18	0.17	0.167
W_b/MJ	175.	84.3	76.6	45.2	31.4	21.5
$L_{AA0}/\text{cm}^{-2}s^{-1}$	9.43×10^{31}	4.33×10^{30}	2.9×10^{30}	3.11×10^{29}	6.66×10^{28}	1.36×10^{28}
$L_{NN0}/\text{cm}^{-2}s^{-1}$	2.41×10^{34}	6.93×10^{33}	4.64×10^{33}	1.89×10^{33}	1.11×10^{33}	5.88×10^{32}
P_{BFPP}/W	0.0199	0.601	0.935	11.	60.6	350.
P_{EMD1}/W	32.	55.6	52.2	78.3	107.	141.
τ_{LD}/h	6.45	11.6	13.1	9.74	4.96	1.57
T_{opt}/h	5.68	7.62	8.08	6.98	4.98	2.8
$\langle L_{AA}\rangle$ $\text{cm}^{-2}s^{-1}$	4.54×10^{31}	2.45×10^{30}	1.69×10^{30}	1.68×10^{29}	2.95×10^{28}	3.8×10^{27}
$\langle L_{NN}\rangle$ $\text{cm}^{-2}s^{-1}$	1.16×10^{34}	3.93×10^{33}	2.71×10^{33}	1.02×10^{33}	4.91×10^{32}	1.64×10^{32}
$\int_{month} L_{AA}$ dt/nb^{-1}	5.89 $\times 10^{4}$	3180.	2190.	218.	38.2	4.92
$\int_{month} L_{NN}$ dt/pb^{-1}	1.51×10^{4}	3090.	3510.	1330.	636.	213.
R_{had}/kHz	1.33×10^{5}	1.12×10^{4}	7540.	1260.	378.	106.
μ	10.6	0.893	0.598	0.1	0.03	0.00842

$$
\begin{aligned}
N_l &= \#\text{ of months} \times \int_{\text{month}} L_{AA}\,dt \\
&\times \text{Centrality Percentage} \\
&\times \sum_{a,b\in p,n} N_{ab}\frac{d\sigma_{ab\to W}}{dMdy} \\
&\otimes \Gamma_{W\to l\nu_l} \times 2 \times \Delta y_l
\end{aligned}
$$

- Assumes 100% efficiency of $W \to e\nu_e, \mu\nu_\mu$, $Z \to e^+e^-, \mu^+\mu_-$.
- Measurements covers $|y < 2.5|$.
- Statistical uncertainty: $N_l \pm \sqrt{N_l}$.

W^+, W^-, Z boson $R_{AA/BB}$

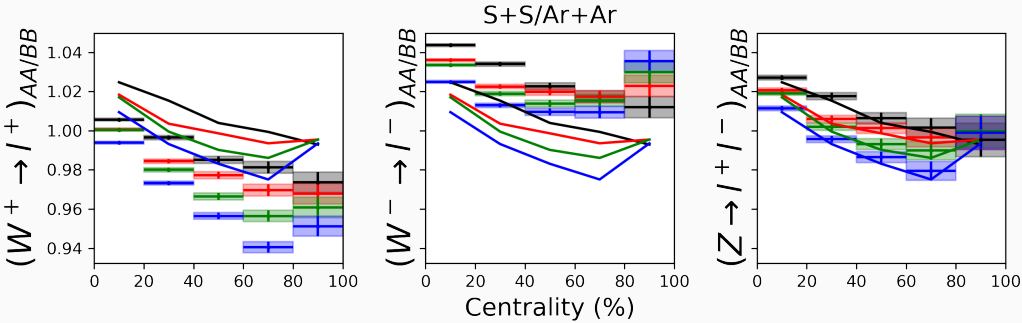

- Lines: N_{coll} vs Centrality.
- Black: $\delta a = 0$. Green: $a_{n,p} = a \pm \delta a$. Red: $a_{n,p} = a \pm \frac{1}{2}\delta a$. Blue: $a_{n,p} = a \pm \frac{3}{2}\delta a$.
- Z boson isobar ratio closely follows the N_{part} scaling remarkably well.

Double ratio $[W^-/W^+]_{AA/BB}$

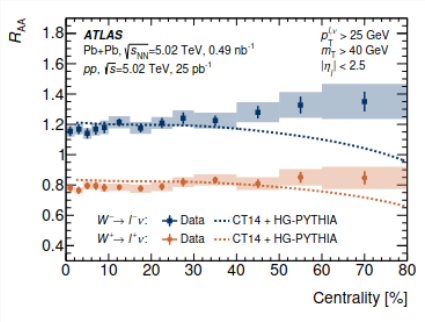

- One can study the double ratio $(W^-/W^+)_{AA/BB}$ or $(W/Z)_{AA/BB}$ to probe the evolution of p/n over centrality (impact parameter).
- Taking W^-/W^+ ratio further cancels biases in peripheral collisions from triggering on a hard process.

Double ratio: $^{36}_{16}S$ vs $^{36}_{18}Ar$

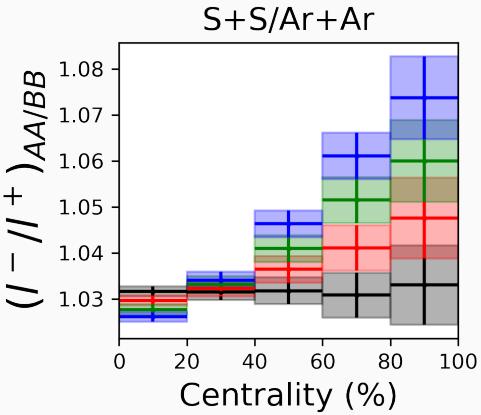

$R = 3.56$ fm, $a = 0.5$ fm, vary δa.

- 3 TeV + 3 TeV, $\sqrt{s} = 6$ TeV, $y_{\rm com} = 0$, $|y_l| < 2.5$.
- Notable increase of double ratio from central to peripheral collisions.
- Green: $a_{n,p} = a \pm \delta a$.
- Red: $a_{n,p} = a \pm \frac{1}{2}\delta a$.
- Blue: $a_{n,p} = a \pm \frac{3}{2}\delta a$.

Double ratio: $^{36}_{16}S$ vs $^{36}_{18}Ar$

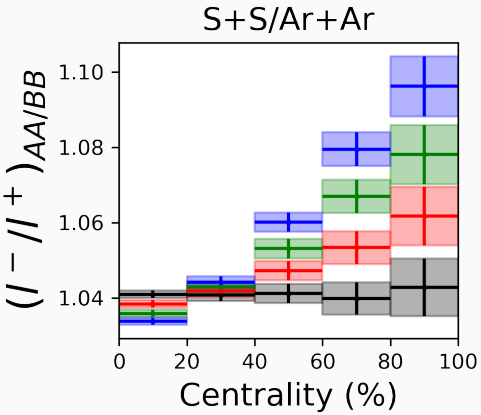

$R = 3.56$ fm, $a = 0.5$ fm, vary δa.

- 3 TeV + 3 TeV, $\sqrt{s} = 6$ TeV, **full rapidity coverage**.
- Notable increase of double ratio from central to peripheral collisions.
- Green: $a_{n,p} = a \pm \delta a$.
- Red: $a_{n,p} = a \pm \frac{1}{2}\delta a$.
- Blue: $a_{n,p} = a \pm \frac{3}{2}\delta a$.

Double ratio: $^{36}_{16}S$ vs $^{36}_{18}Ar$

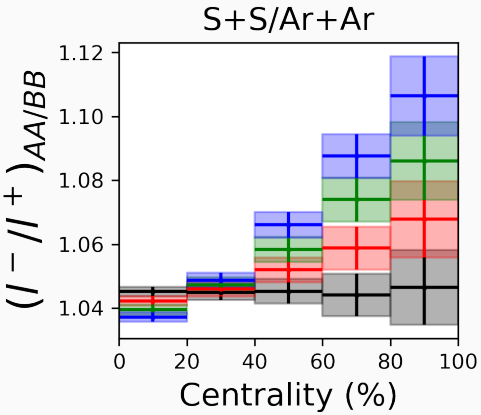

$R = 3.56$ fm, $a = 0.5$ fm, vary δa.

- **3 TeV + 1 TeV**, $\sqrt{s} = 3.46$ TeV, $y_{\rm com} = 0.55$, $|y_l| < 2.5$.
- Notable increase of double ratio from central to peripheral collisions.
- Green: $a_{n,p} = a \pm \delta a$.
- Red: $a_{n,p} = a \pm \frac{1}{2}\delta a$.
- Blue: $a_{n,p} = a \pm \frac{3}{2}\delta a$.

Double ratio: $^{48}_{20}Ca$ vs $^{48}_{22}Ti$

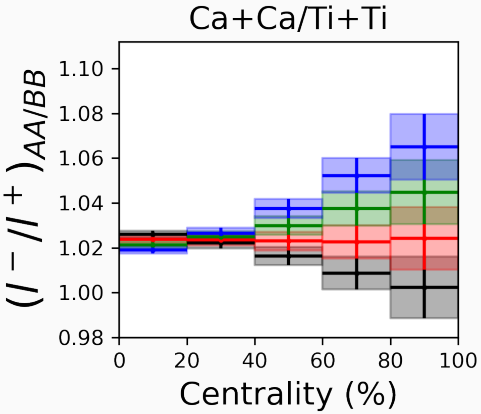

- $\sqrt{s} = 6$ TeV, $y_{\rm com} = 0$, $|y_l| < 2.5$.
- Varing δa for Ca.

$R = 3.92$ fm, $a = 0.5$ fm, changing a_p, a_n

Double ratio: $^{48}_{20}Ca$ vs $^{48}_{22}Ti$

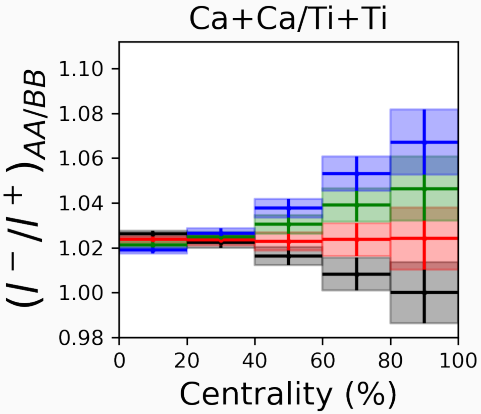

$R = 3.92$ fm, $a = 0.45$ fm, changing a_p, a_n

- $\sqrt{s} = 6$ TeV, $y_{\rm com} = 0$, $|y_I| < 2.5$.
- Varing δa for Ca.
- The double ratio is no longer sensitive to isospin insensitive parameters.
  $a_{\rm Ca}$: 0.5 $\rightarrow$ 0.45 fm, increase d to maintain the same neutron skin thickness.

Double ratio: $^{48}_{20}Ca$ vs $^{48}_{22}Ti$

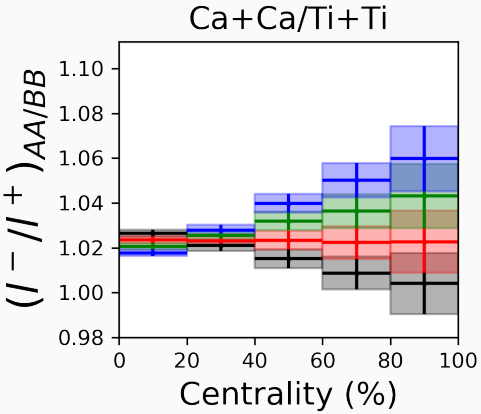

$R = 3.92$ fm, $a = 0.5$ fm, changing R_p, R_n

- $\sqrt{s} = 6$ TeV, $y_{\rm com} = 0$, $|y_I| < 2.5$.
- Varing δa for Ca.
- The double ratio is no longer sensitive to isospin insensitive parameters.
  $a_{\rm Ca}$: $0.5 \rightarrow 0.45$ fm, increase d to maintain the same neutron skin thickness.
- Change R instead of a.

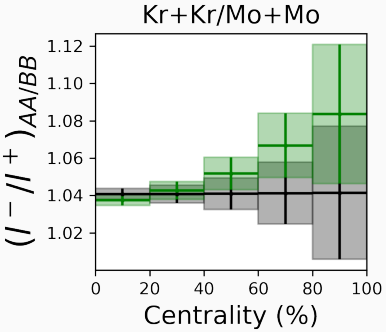

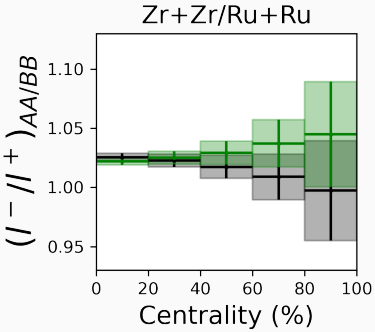

- $\sqrt{s} = 6$ TeV, $y_{\mathrm{com}} = 0$, $|y_l| < 2.5$.
- Currently still limited by luminosity.
- Explore other isospin sensitive probes, e.g., jet charge; in UPC events?
- Future Circular Collider?

Z boson isobar ratio: hard collision input

- $0 < \beta_{2,\mathrm{Ru}}, \beta_{2,\mathrm{Zr}} < 0.35$.
- $0 < \beta_{3,\mathrm{Ru}}, \beta_{3,\mathrm{Zr}} < 0.35$.
- $4.9 < R_{\mathrm{Ru}}, R_{\mathrm{Zr}} < 5.1$ fm.
- $0.4 < a_{\mathrm{Ru}}, a_{\mathrm{Zr}} < 0.6$ fm.
- $-0.1 < p < 0.1$, from early studies.
- $0.4 < w < 1.0$ fm, nucleon width.
- $1/3 < k < 3$, fluctuation.
- $0 < d < 1.5$ fm, repulsion.

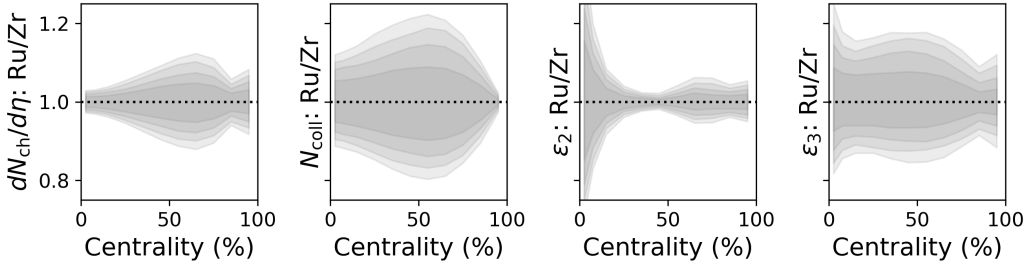

Isobar results from STAR Collaboration [arXiv:2109.00131]

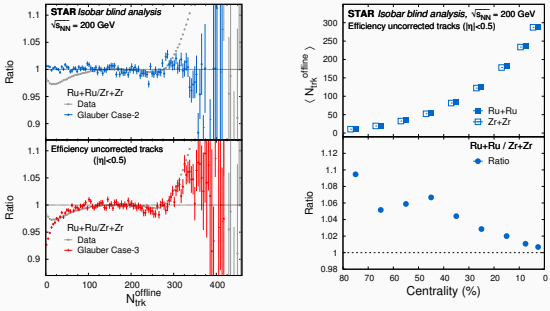

- Very high precision measurements: multiplicity, flow, etc.
- Still challenging for models of final-state interaction. Previous Global fits usually agree with multiplicity and flow data within 5-10% uncertainty.
- Independent input from hard scatterings can be useful.

Binary collision + flow ratios

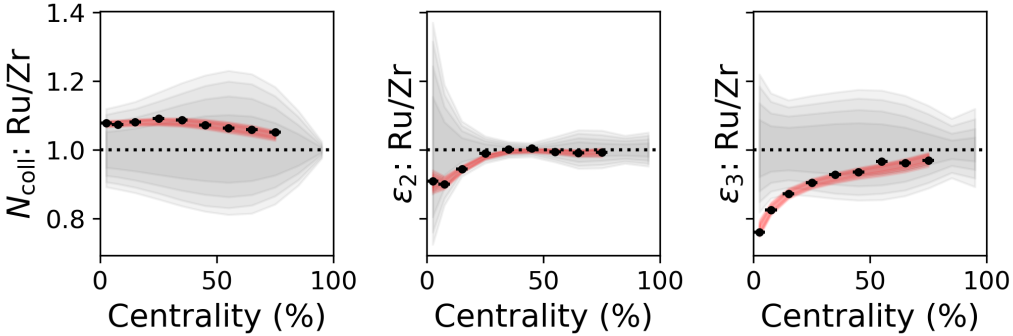

Binary collision + flow ratios: woods-Saxon parameters

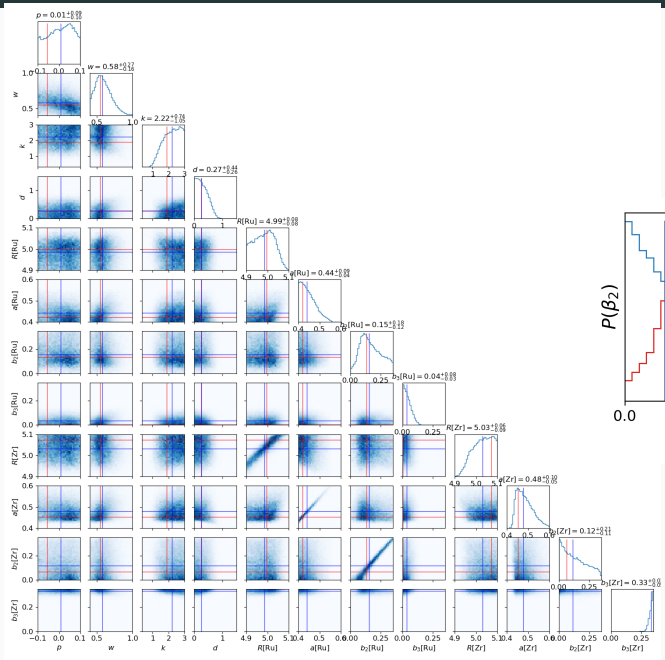

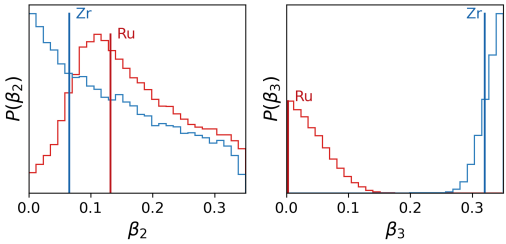

Summary

- Hard probes N_{coll} have different scaling from soft hadron production $\approx N_{\mathrm{part}}$, Z-boson isobar ratios can be used as independent inputs to constrain initial condition model.
- $W^{\pm}$ are very clean probes of isospin differences of isobar pairs.
- The centrality dependent isobar double ratio $(W^{-}/W^{+})_{AA/BB}$ probes neutron skin and cancels a large fraction of theory and modeling uncertainty.
- May be viable for light nuclei at HL-LHC (e.g., S vs Ar, Ca vs Ti), heavy nuclei are limited by statistics.
- Jets/hadrons: isobar ratio of self normalized new observables, study path-length distributions.

Questions?

Nuclear/nucleon configurations & total cross-section

Centrality: percentage of minimum-bias hadronic cross section Pb-Pb@2.76 TeV $770 \pm 10(\text{stat.})^{+60}_{-50}(\text{sys.})\text{fm}^2$ **8% level**. [ALICE PRL 109 252302, PRC 88 044909].

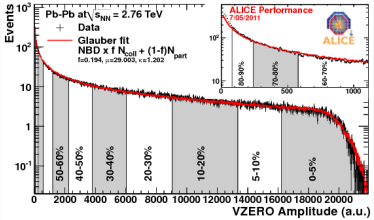

In Glauber-based models, including TRENTo

- Gaussian nucleon w and β can affect the total cross section: $\sigma_{\text{PbPb}}^{\text{TRENTo}}[w = 0.5\ \text{fm}] = \mathbf{782 \pm 4}\ \text{fm}^2$ vs $\sigma_{\text{PbPb}}^{\text{TRENTo}}[w = 0.8\ \text{fm}] = \mathbf{833 \pm 4}\ \text{fm}^2$
- Some reasons that σ_{AA} is not used as a constraint in analysis before:
  - *pp* and nuclear inelastic cross-section have large uncertainty.
  - No exact match of geometry model to the experimental minimum-bias trigger.
  - Different IC models have different minimum-bias criteria ...
- Can we make use of the precision measurement cross sections in isobar collisions?

Isobar double ratios

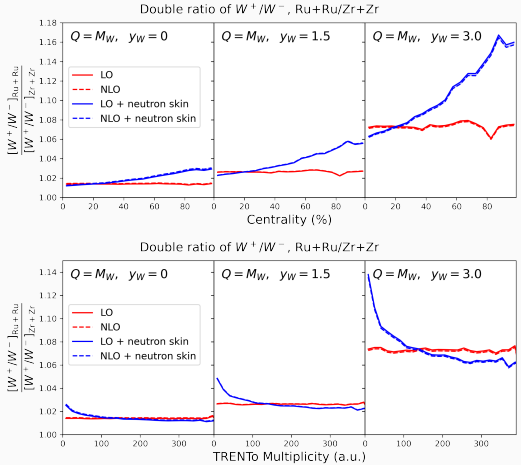

*Nuclear PDF uncertainty not shown.

Larger difference at

1. large rapidity $\rightarrow$ valance region.
2. peripheral (the skin) collisions $\rightarrow$ significantly lower *NN* luminosity.

W^+, W^-, Z **boson** $R_{AA/BB}$

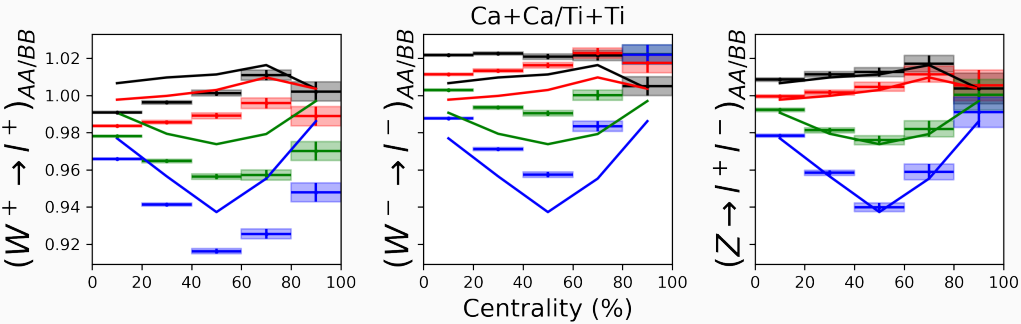

W^+, W^-, Z **boson** $R_{AA/BB}$

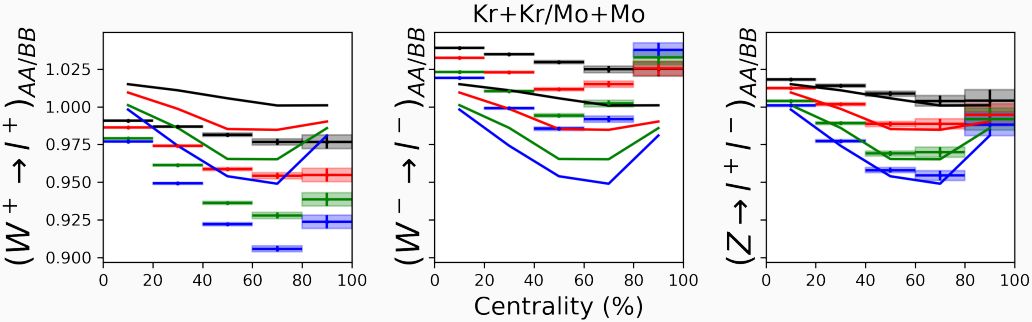
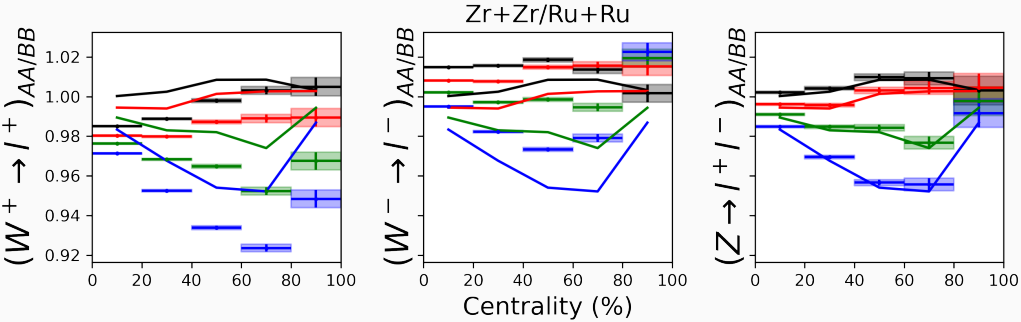
W^+, W^-, Z **boson** $R_{AA/BB}$